On the Method of Logarithmic Cumulants for Parametric Probability Density Function Estimation

Vladimir Krylov, Gabriele Moser, Sebastiano B. Serpico, Josiane Zerubia

▶ To cite this version:

Vladimir Krylov, Gabriele Moser, Sebastiano B. Serpico, Josiane Zerubia. On the Method of Logarithmic Cumulants for Parametric Probability Density Function Estimation. [Research Report] RR-7666, INRIA. 2011. inria-00605274v2

HAL Id: inria-00605274
https://inria.hal.science/inria-00605274v2

Submitted on 16 Aug 2011

INRIA

On the Method of Logarithmic Cumulants for Parametric Probability Density Function Estimation

Vladimir A. Krylov   — Gabriele Moser   — Sebastiano B. Serpico   — Josiane Zerubia

N° 7666

July 2011

Vision, Perception and Multimedia Understanding

Rapport de recherche

On the Method of Logarithmic Cumulants for Parametric Probability Density Function Estimation

Vladimir A. Krylov [*] [†] , Gabriele Moser [‡] [§] , Sebastiano B. Serpico [‡] [¶] , Josiane Zerubia [*] [‖]

Abstract: Parameter estimation of probability density functions is one of the major steps in the mainframe of statistical image and signal processing. In this report we explore the properties and limitations of the recently proposed method of logarithmic cumulants (MoLC) parameter estimation approach which is an alternative to the classical maximum likelihood (ML) and method of moments (MoM) approaches. We derive the general sufficient condition of strong consistency of MoLC estimates which represents an important asymptotic property of any statistical estimator. With its help we demonstrate the strong consistency of MoLC estimates for a selection of widely used distribution families originating (but not restricted to) synthetic aperture radar (SAR) image processing. We then derive the analytical conditions of applicability of MoLC to samples generated from several distribution families in our selection. Finally, we conduct various synthetic and real data experiments to assess the comparative properties, applicability and small sample performance of MoLC notably for the generalized gamma and K family of distributions. Supervised image classification experiments are considered for medical ultrasound and remote sensing SAR imagery. The obtained results suggest MoLC to be a feasible yet not universally applicable alternative to MoM that can be considered when the direct ML approach turns out to be unfeasible.

[*] EPI Ariana, CR INRIA Sophia Antipolis Méditeranée, 2004, Route des Lucioles, B.P.93, F-06902, Sophia Antipolis Cedex (France)

[†] e-mail: Vladimir.Krylov@inria.fr

[‡] Dept. of Biophysical and Electronic Engineering (DIBE), University of Genoa, Via Opera Pia 11a, I-16145, Genoa (Italy)

[§] e-mail: gabriele.moser@unige.it

[¶] e-mail: sebastiano.serpico@unige.it

[‖] e-mail: Josiane.Zerubia@inria.fr

Sur la méthode des cumulants logarithmiques pour l'estimation des fonctions de densité de probabilité paramétriques

Résumé : L'estimation de paramètres de fonctions de densité de probabilité est une étape majeure dans le domaine du traitement statistique du signal et des images. Dans ce rapport, nous étudions les propriétés et les limites de l'estimation de paramètres par la méthode des cumulants logarithmiques (MoLC), qui est une alternative à la fois au maximum de vraisemblance (MV) classique et à la méthode des moments. Nous dérivons la condition générale suffisante de consistance forte de l'estimation par la méthode MoLC, qui représente une propriété asymptotique importante de tout estimateur statistique. Grâce à cela, nous démontrons la consistance forte de l'estimation par la méthode MoLC pour une sélection de familles de distributions particulièrement adaptées (mais non restreintes) au traitement d'images acquises par radar à synthèse d'ouverture (RSO). Nous dérivons ensuite les conditions analytiques d'applicabilité de la méthode MoLC à des échantillons générés à partir des différentes familles de distribution de notre sélection. Enfin, nous testons la méthode MoLC sur des données synthétiques et réelles, afin de comparer les différentes propriétés inhérentes aux différents types d'images, l'applicabilité de la méthode et les effets d'un nombre restreint d'échantillons. Nous avons, en particulier, considéré les distributions gamma généralisée et K. Comme exemple d'application, nous avons réalisé des classifications supervisées d'images médicales ultrason ainsi que d'images de télédétection acquises par des capteurs RSO. Les résultats obtenus montrent que la méthode MoLC est une bonne alternative à la méthode des moments, bien qu'elle contienne certaines limitations. Elle est particulièrement utile lorsqu'une approche directe par MV n'est pas possible.

Mots-clés : Densité de probabilité, estimation de paramètres, classification, image radar, RSO, image haute résolution, image médical ultrason, consistance forte, distribution gamma généralisée, K distribution.

Contents

1   Introduction

Parameter estimation of probability density functions (pdfs) is a topic of vital importance in pattern recognition, image and signal processing. Many real-time signal processing applications require automatic, stable and statistically consistent methods for the characterization of the underlying signals. In the mainframe of basic image processing applications, such as segmentation and classification, obtaining the parameter estimates is the classical problem encountered while employing statistical approaches [1].

The classical methods of statistical parameter estimation include the maximum likelihood (ML) and the method of moments (MoM) [2]. The ML approach suggests to choose the parameter values that provide the highest value of the likelihood function by, typically, finding the appropriate root of the likelihood function derivative. This simple yet powerful estimation strategy is widely used and its theoretical statistical properties are well established under some regularity conditions [2]. However, in a wide class of applications the considered pdf models involve complicated analytical expressions and do not originate from the exponential family of distributions and, as such, fail to comply with the classical regularity conditions that guarantee the attractive asymptotical properties of ML estimates such as, first of all, asymptotic consistency and efficiency. Furthermore, ML procedures are notorious for their considerable computational load that originates from expressions not allowing analytical formulations and, thus, often involving intensive numerical procedures sensitive to initialization. For some distribution families the ML approach does not allow to formulate a well established and reliable parameter estimation procedure [3, 4, 5, 6]. Approximate iterative ML estimation methods are frequently used, in particular, the Expectation Maximization approach [7] and its modifications.

The second generally used parameter estimation procedure is given by MoM. This method is based on the idea of formulating the theoretical moments $\mathbb{E}X^k$ of the considered random variable X as functions of its unknown parameters via the Laplace transform and setting them equal to the observed sample moments, thus, obtaining a system of equations with respect to parameters [2]. Outperformed by ML in simple and well studied cases, such as, e.g., the exponential family of distributions including most popular Gamma and Gaussian pdfs [2], the MoM strategy often enables to obtain feasible and fast estimates in cases where ML fails or cannot perform in real-time [5, 8]. However this method suffers from its own limitations [2]. First, the applicability of this method is restricted by the existence of finite moments up to the necessary order which is not the case in some critical cases. Second, based on high order statistics MoM can be very sensitive to outliers that are inherent in real signals due to noise or registration faults. Finally, similar to ML, the Laplace transform can bring to some complicated expressions which result in a system of implicit MoM equations that may not allow analytical inversion, thus, resulting in the same numerical and initialization problems, see, e.g., [3]. To address some of these issues, various modifications of MoM have been developed, including negative, fractional moments methods and generalized MoM (see [2] and below).

In this report we study the use of the method of logarithmic cumulants (MoLC) parameter estimation approach that has been first introduced by J.-

M. Nicolas in [8][1]. Contrary to the classical estimation methods based on the use of Laplace and Fourier transforms that are not well adapted for pdfs on $\mathbb{R}^+ = (0, +\infty)$, MoLC is a parameter estimation technique developed specifically for positive valued pdfs. Employing a strategy somewhat similar to MoM, this method is based on the use of the Mellin integral transform. It has been observed [9] that the use of Mellin transform is a natural analytical tool in studying the distributions of products of random variables, which tends to be a frequent case in signal processing applications [8]. More specifically, in case of some random variables with complicated pdf expressions, MoLC, unlike ML and MoM, enables to obtain systems of equations which allow analytical solutions, e.g., for the heavy-tailed Rayleigh pdf [8, 10], or a simple numerical estimation procedure, as is the case with the generalized gamma distribution (GΓD) [11] and K-distribution [12]. For this reason MoLC found many applications in synthetic aperture radar (SAR) image processing [13]. SAR sensors operate in the domain of microwaves and enable to obtain regular high-resolution imagery that represents an important source of information in remote sensing applications. Being registered by an active imaging system, SAR images suffer from the inherent multiplicative noise known as speckle, which originates from the interference of the coherent wavefronts [13]. Most SAR-specific statistical models take into account speckle and, therefore, constitute multiplicative models, which renders them well suited for the Mellin transform and MoLC. It is important, though, that the area of applications of MoLC is not exhausted by SAR image processing problems. For example, in the latter we will investigate the properties of MoLC as applied: to the GΓD pdf family, which is a universal statistical model that is employed in, e.g., speech [14] and image processing [3, 15], and to the K distribution, that found its place in a wide class of scattered signal processing problems [6].

The aim of this work is to further explore the properties and limitations of the MoLC approach, conduct new relevant comparisons and study the small sample performance of this estimator as applied to image processing problems. To this end, we consider the use of MoLC parameter estimator for the selection of statistical models presented in Table 1. These pdf models constitute a representative selection of models employed in statistical SAR image processing, see [13, 5, 16]. Above all, we concentrate on the above mentioned GΓD and K models since their application areas are not restricted to SAR.

The contribution of this report is threefold. First, we establish a general set of sufficient conditions for the strong consistency property of MoLC and then use it to demonstrate this property of MoLC estimates for the considered selection of pdf families. We stress that the demonstrated property is an important characteristic of any statistical estimator that guarantees its almost sure convergence to the true parameter values as the sample-size grows [2]. We consider the proofs of strong consistency to be a worthwhile contribution since they guarantee from the theoretical point of view the good statistical properties of MoLC estimation results. To the best of our knowledge, up to now it is only the consistency of MoLC estimates for the generalized Gaussian-Rayleigh that has been demonstrated [4]. Second, we derive the analytical conditions of MoLC applicability to GΓD, K and Fisher models, which is complementary to the visual representation

---

[1]The original paper is written in French, yet its translation into English, prepared by S.N. Anfinsen, can be found online at *http://eo.uit.no/publications/JMN-TRANS-10.pdf*

of these conditions reported previously in [8, 5, 17]. The third contribution is the experimental study of the MoLC approach where we conduct new synthetic and real-data experiments in order to analyze the comparative and small sample performance as well as the applicability of the MoLC approach. As applied to image processing, we consider the performance of MoLC for the supervised classification of speckled imagery, such as medical ultrasound and remote sensing SAR.

The report is organized as follows. In Section 2 we briefly summarize some important results previously obtained in the literature on MoLC estimation applied to pdf families in the selection given by Table 1. In Section 3 we present the MoLC parameter estimation strategy. In Section 4 we prove novel sufficient condition of MoLC estimator's strong consistency and employ it to demonstrate the MoLC estimates' strong consistency for the families involved in this study. In Section 5 we derive the applicability restrictions of MoLC estimator to several pdf models. In Section 6 we perform synthetic-data comparisons of MoLC with alternative estimation techniques for GΓD and K-law. In Section 7 we perform real-data experiments with ultrasound and SAR imagery. Finally, in Section 8 we draw the conclusions of this study.

Table 1: Pdfs and MoLC equations for the considered pdf families. Here $\Gamma(\cdot)$ is the Gamma function [18], $K_\alpha(\cdot)$ the αth order modified Bessel function of the second kind [18], $J_0(\cdot)$ is the zero-th order Bessel function of the first kind [18], $\Psi(\nu, \cdot)$ the νth order polygamma function [18] and $G_\nu(\cdot)$ are the specific integral functions for GGR [4]

Family	Probability density function	MoLC equations
Generalized Gamma (GGD) [11, 14, 15, 3, 17]	$f_{\nu,\kappa,\sigma}(r) = \frac{|\nu|}{\sigma\Gamma(\kappa)} \left(\frac{r}{\sigma}\right)^{\kappa\nu-1} \exp\left[-\left(\frac{r}{\sigma}\right)^\nu\right]$, $\quad \nu \neq 0, \quad \kappa, \sigma > 0, \quad r > 0$	$k_1 = \Psi(0,\kappa)/\nu + \ln\sigma$ $\quad k_j = \Psi(j-1,\kappa)/\nu^j, \quad j = 2,3$
Lognormal [13]	$f_{m,\sigma}(r) = \frac{1}{\sigma r\sqrt{2\pi}} \exp\left[-\frac{(\ln r - m)^2}{2\sigma^2}\right], \quad m \in \mathbb{R}, \sigma > 0, \quad r > 0$	$k_1 = m \quad k_2 = \sigma^2$
Weibull [13]	$f_{\eta,\mu}(r) = \frac{\eta}{\mu^\eta} r^{\eta-1} \exp\left[-\left(\frac{r}{\mu}\right)^\eta\right], \quad \eta, \mu > 0, \quad r \geq 0$	$k_1 = \ln\mu + \eta^{-1}\Psi(0,1) \quad k_2 = \eta^{-2}\Psi(1,1)$
Gamma [13, 8]	$f_{L,\mu}(r) = \frac{1}{\Gamma(L)} \left(\frac{L}{\mu}\right)^L r^{L-1} \exp\left[-\frac{Lr}{\mu}\right], \quad L, \mu > 0, \quad r \geq 0$	$k_1 = \Psi(0,L) + \ln\mu - \ln L \quad k_2 = \Psi(1,L)$
Nakagami [13, 8]	$f_{L,\lambda}(r) = \frac{2}{\Gamma(L)} (\lambda L)^L r^{2L-1} \exp[-\lambda L r^2], \quad L, \lambda > 0, \quad r \geq 0$	$2k_1 = \Psi(0,L) - \ln\lambda - \ln L \quad 4k_2 = \Psi(1,L)$
Fisher [8, 5, 19]	$f_{\mu,L,M}(r) = \frac{\Gamma(L+M)}{\Gamma(L)\Gamma(M)} \frac{[Cr]^L}{r[1+Cr]^{L+M}}$, $\quad C = \frac{L}{M\mu}, \quad \mu, L, M > 0, \quad r > 0$	$k_1 = \ln\mu + (\Psi(0,L) - \ln L) - (\Psi(0,M) - \ln M)$ $\quad k_j = \Psi(j-1,L) + (-1)^j\Psi(j-1,M), \quad j = 2,3$
K-distribution [12, 6]	$f_{\mu,L,M}(r) = \frac{2}{\Gamma(L)\Gamma(M)} r^{\frac{L+M}{2}-1} C^{L+M} K_{M-L}\left(2Cr^{1/2}\right)$, $\quad C = \left(\frac{LM}{\mu}\right)^{1/2}, \quad \mu > 0, 0 < L < M, \quad r \geq 0$	$k_1 = \ln\mu + \Psi(0,L) + \Psi(0,M) - \ln LM$ $\quad k_j = \Psi(j-1,L) + \Psi(j-1,M), \quad j = 2,3$
K-root distribution [12, 6]	$f_{\mu,L,M}(r) = \frac{4}{\Gamma(L)\Gamma(M)} r^{L+M-1} C^{L+M} K_{M-L}(2Cr)$, $\quad C = \left(\frac{LM}{\mu}\right)^{1/2}, \quad \mu > 0, 0 < L < M, \quad r \geq 0$	$2k_1 = \ln\mu + \Psi(0,L) + \Psi(0,M) - \ln LM$ $\quad 2^j k_j = \Psi(j-1,L) + \Psi(j-1,M), \quad j = 2,3$
Generalized Gaussian - Rayleigh (GGR) [4, 16]	$f_{\lambda,\gamma}(r) = \frac{\gamma^2 r}{\lambda^2\Gamma^2(\lambda)} \int_0^{\pi/2} \exp\left[-(\gamma r)^{\frac{1}{\lambda}}\left(|\cos\theta|^{\frac{1}{\lambda}} + |\sin\theta|^{\frac{1}{\lambda}}\right)\right] d\theta$, $\quad \lambda, \gamma > 0, \quad r \geq 0$	$k_1 = \lambda\Psi(0,2\lambda) - \ln\gamma - \lambda G_1(\lambda)[G_0(\lambda)]^{-1}$ $\quad k_2 = \lambda^2\left[\Psi(1,2\lambda) + \frac{G_2(\lambda)}{G_0(\lambda)} - \left(\frac{G_1(\lambda)}{G_0(\lambda)}\right)^2\right]$
Heavy-tailed Rayleigh [10, 8]	$f_{\alpha,\gamma}(r) = r \int_0^{+\infty} \rho \exp[-\gamma\rho^\alpha] J_0(r\rho) d\rho$, $\quad \alpha, \gamma > 0, \quad r \geq 0$	$\alpha k_1 = (\alpha-1)\Psi(0,1) + \ln\gamma 2^\alpha$ $\quad k_2 = \alpha^{-2}\Psi(1,1)$

2 Previous work on MoLC

In this section we recall some relevant results previously obtained in the literature on the MoLC parameter estimation technique applied to the pdf families presented in Table 1.

First we recall the results obtained for the GΓD and its subfamilies. The use of MoLC for GΓD has been advocated in [17][2] in order to address the arising complicated parameter estimation problem and has demonstrated good comparative performance for SAR statistics modeling. The theoretical aspects of MoLC approach have not been previously investigated and will be addressed in this report. Some research has been performed concerning the subfamilies of GΓD. The theoretical analysis of the Gamma distribution performed in [8] demonstrated the lower variance of shape parameter L estimates obtained by MoLC than by MoM yet somewhat above the variance of lower order moments (LOM) method. However, due to optimal order estimation problem for LOM, the MoLC approach is preferable for the estimation of shape parameter. In [5] a panel of experiments was performed to analyze the performance of MoLC to the Nakagami distribution: Experimental comparisons demonstrating lower level of estimates' mean square errors obtained via MoLC as compared to ML and MoM for samples of moderate size ($N = 1000$). It is important to notice that the Gamma and Nakagami distributions have a strong connection, more specifically, if the random variable X follows the Gamma law, then $\sqrt{X}$ is Nakagami-distributed (see Table 1). Therefore, the above mentioned results are closely connected.

Further important results were obtained in [8, 5, 19] for the Fisher pdf family. It has been observed that the ML method does not automatically constitute the best parameter estimation strategy since one cannot claim the minimum variance unbiased property as is the case with the classical gamma distribution [19]. Therefore, the MoLC estimation strategy has been compared in [5, 19] with MoM and the mixed estimation method, based on mixed moments $\mathbb{E}[X^s \log X]$. Several interesting observations have been obtained. First, the applicability of moment and mixed moment methods is restricted by the existence of the employed moments, which corresponds to $M > 2$ for moments and $M > 3$ for the mixed moment approaches. Second, the acceptance rate of the obtained estimates was analyzed to evaluate their applicability, i.e. whether these estimates are positive and, therefore, can be utilized to construct a Fisher distribution. MoLC has demonstrated a 100% acceptance rate, notably for small size samples, which significantly outperformed the (mixed) moment-based methods. Finally, for small values of M the experimentally observed values of the Kullback-Leibler divergence between the true and estimated pdfs obtained by the MoLC approach were appreciably smaller than the ones acquired with (mixed) moment-based methods. These observations confirm the strong applicability and comparative efficiency of the MoLC approach to the Fisher family of distributions. It is worth noticing that the Inverse Gaussian model $\mathcal{G}_0$ (see in [5]) coincides with the Fisher pdf family and, as such, the same results apply.

The use of MoLC for the K and K-root distributions [12] has been suggested in [8]. As can be seen in Table 1, these distribution families are closely connected: K-root gives the distribution of a random variable $\sqrt{X}$, when X

---

[2]More specifically, the GΓD model adapted by Li et al. in [17] is slightly different from the classical GΓD, see [11, 3], adapted in this report. Nevertheless, most of the obtained results extend to both formulations.

follows the K-distribution. The advantage of MoLC is that it brings to simpler expressions than MoM, as is typically the case with multiplicative models, and, furthermore, the ML approach is not directly applicable. MoLC properties as applied to K and K-root families will be further addressed below.

In case of the GGR model the ML approach is not feasible since the likelihood function contains several integral summands that cannot be treated analytically and render the numerical maximization very costly [4]. MoLC estimates stability for GGR has been validated in [4] in case of varying sample size. The applicability of MoLC for GGR is restricted by a certain condition on the sample second-order logarithmic cumulant, otherwise the system of MoLC equations has no solution (see in [4]). The heavy-tailed Rayleigh distribution (equivalent to Rayleigh-mixture) was proposed in [10] for SAR images along with the corresponding negative order moment procedure for parameter estimation. This procedure has been developed since the usual moments are not defined from order $\min(\alpha, 2)$ and upwards (see Table 1). The applicability of the MoLC method to this model has been demonstrated in [8] and the corresponding equations were derived. One can notice that the MoLC equations allow a simple analytical solution (see Table 1) whereas the method proposed in [10] involves numerical approximations.

Finally, it is worth noticing that the experiments conducted with the multivariate matrix-equivalent of MoLC [20], i.e. method developed based on the matrix-variate Mellin transform, to several state-of-the-art polarimetric SAR complex-valued pdf families have demonstrated superior bias and variance properties than the original moment-based parameter estimation methods. As in the single-variate case Mellin kind statistics, the mathematical tractability and the simplicity of the obtained expressions [20] show that the extension of MoLC to matrix-valued data is a well-adapted and accurate tool for multilook polarimetric radar data.

3   Method of Logarithmic Cumulants

In this section we recall the method of logarithmic cumulants (MoLC) approach following the general notations introduced in [8].

MoLC is a parameter estimation technique developed for pdfs defined on $\mathbb{R}^+$. Based on the Mellin integral transform it is well-suited for distributions defined as products of random variables [9], which is a frequent case in signal processing applications including signals collected by active acquisition systems such as radar and sonar in remote sensing [13] and ultrasound in medical imaging [21]. Therefore, as demonstrated in [8], the use of Mellin transform makes it possible to perform a more effective analysis of practically important distributions defined on $\mathbb{R}^+$.

Let X be a positive-valued random variable with pdf $p(u)$ defined on $u \in \mathbb{R}^+$. The Mellin transform of $p(u)$ is defined as

$$\phi(t) = \int_0^{+\infty} u^{t-1} p(u) du, \tag{1}$$

where the integral converges for t in an open vertical strip of the complex plane and $\phi(t)$ is analytical inside this convergence strip. Following the notations introduced in [8], this transform $\phi(t)$ is referred to as the first characteristic

function of the second kind. The inverse Mellin transform, which enables to retrieve $p(u)$ from $\phi(t)$ is given by

$$p(u) = \frac{1}{2\pi i} \int_{c-i\infty}^{c+i\infty} u^{-t} \phi(t) dt.$$

The second kind moment (log-moment) of order $s \in \mathbb{N}$ is defined as

$$\tilde{m}_s = \left.\frac{\mathrm{d}^s}{\mathrm{d}t^s}\phi(t)\right|_{t=1} = \int_0^{+\infty} (\ln u)^s p(u) du \tag{2}$$

where the second equality follows from the properties of the Mellin transform [8].

One then defines the second characteristic function of the second kind as the natural logarithm of the first characteristic function of the second kind:

$$\psi(t) = \ln \phi(t)$$

and its derivatives as the second kind cumulants (log-cumulants):

$$\tilde{k}_s = \left.\frac{\mathrm{d}^s}{\mathrm{d}t^s}\psi(t)\right|_{t=1}. \tag{3}$$

Analytically, second kind cumulants are constructed in the same way as the traditional cumulants and, therefore, the same relations between log-cumulants and log-moments hold as in the case of classical moments and cumulants [2]. For instance, the first three log-cumulants can be written as:

$$\tilde{k}_1 = \tilde{m}_1$$
$$\tilde{k}_2 = \tilde{m}_2 - \tilde{m}_1^2$$
$$\tilde{k}_3 = \tilde{m}_3 - 3\tilde{m}_1\tilde{m}_2 + 2\tilde{m}_1^3.$$

According to the sufficient condition proposed in [8], to ensure the existence of log-moments and log-cumulants of arbitrary orders it suffices to verify that the point $t = 1$ lies inside the convergence strip of the second kind characteristic function (1).

If we denote the Fourier transform of the pdf of a random variable Y as $\Phi_Y(t)$ we obtain [8] ($v \in \mathbb{R}$):

$$\Phi_{\ln X}(v) = \left.\phi_X(t)\right|_{t=1+iv}. \tag{4}$$

In other words, finding the Mellin transform (characteristic function of the second kind) is equivalent to deriving the expression for the Fourier transform (ordinary characteristic function) in the logarithmic scale. Therefore, log-moments and log-cumulants can be obtained by differentiating (4).

Taking into account the property given by (2) we get

$$\tilde{k}_1 = \mathbb{E} \ln X$$
$$\tilde{k}_s = \mathbb{E}\left[\ln X - \tilde{k}_1\right]^s$$

for integer $s \geqslant 2$. If we then combine the definition (3) with the sample estimates of central moments [22] obtained on i.i.d. observations $\{x_i\}_{i=1}^n$, with $x_i \sim X$, we can deduce the following relations:

$$
\begin{aligned}
\tilde{k}_1 &= \frac{\mathrm{d}}{\mathrm{d}t} \ln \phi(t) \Big|_{t=1} \approx \hat{k}_{1n} = \frac{1}{n} \sum_{i=1}^n \ln x_i \\
\tilde{k}_s &= \frac{\mathrm{d}^s}{\mathrm{d}t^s} \ln \phi(t) \Big|_{t=1} \approx \hat{k}_{sn} = \frac{1}{n} \sum_{i=1}^n \left[\ln x_i - \hat{k}_{1n} \right]^s.
\end{aligned}
\tag{5}
$$

This system of equations defines MoLC and provides a method to estimate the parametric pdf models given observations by expressing the characteristic function of the second kind as the function of pdf parameters and then inverting it.

4 Strong consistency of MoLC estimates

4.1 Sufficient conditions

In this section we analyze the statistical asymptotic property of strong consistency for the MoLC estimator by, first, developing a sufficient condition of consistency and, then, proceeding to the strong consistency. We notice that earlier it is only for the GGR model (see [4]) that the MoLC estimates consistency has been proved. The considered property of strong consistency is an important statistical characteristic which, in practice, means that, with probability one, for any admissible sample the sequence of estimates generated by MoLC converges to the true parameter values. By "admissible" we refer to samples for which the MoLC estimator is applicable for a given distribution; this problem is analyzed in detail in Section 5.

Let $p_\xi(x)$ $(x > 0)$ be a family of pdfs defined over $\mathbb{R}^+$ and parameterized by a vector ξ of M real-valued parameters, which takes values in a set $\Xi \subset \mathbb{R}^M$. Let system of MoLC-equations (5) defines a mapping $\Theta : \xi \to k$. Before proceeding to the statements of this section, we first introduce the following three underlying assumptions:

A For each $\xi \in \Xi$, the convergence strip of the Mellin transform of $p_\xi(\cdot)$ includes a neighborhood of unity.

B The vector $\hat{k}_n = (\hat{k}_{1n}, \dots, \hat{k}_{Mn})$ of the first M sample log-cumulants computed on the observed samples $\{x_1, \dots, x_N\}$ is admissible, i.e. $\hat{k}_n \in \Theta(\Xi)$.

C Mapping Θ is injective on Ξ.

Assumption A guarantees the existence of log-cumulants of all orders, Assumption B ensures the applicability of the MoLC approach to the specific sample, and Assumption C allows to recover a unique solution of (5).

Theorem 1. *If Assumptions A, B and C hold, and the inverse of the mapping defined by the system of MoLC equations (5) is continuous at the true parameter value ξ^*, then the sequence $\{\hat{\xi}_n\}$ provides a consistent estimate of ξ^* or, in other words:*

$$
\hat{\xi}_n \to \xi^* \quad \text{in probability.}
$$

A stronger version of consistency property is given by the following theorem.

Theorem 2. *Under the same conditions as in Theorem 1 the MoLC estimator $\{\hat{\xi}_n\}$ provides strongly consistent estimates of ξ^*, or, in other words:*

$$\hat{\xi}_n \to \xi^* \quad almost\ surely.$$

The difference in the statements given by these two theorems allows the following explanation: The consistency guarantees that with the growing sample size the probability of observing a particular sample for which the estimates are "far" from the true parameter values (the difference is larger than any positive ε) is fading to zero. On the other hand, the strong consistency ensures that if we take any initial sample and start consecutively adding new observations to this sample then, with probability one, we obtain a sequence of estimates converging to the true parameter values. The second constitutes a stronger property [22], and, therefore, the result of Theorem 1 follows from Theorem 2. Nevertheless, we consider it important to give both proofs, which are presented in Appendix A, since each of them is based solely on the respective classical moment property.

The previous theorem ensures the strong consistency of the MoLC technique under Assumptions A, B and C, and provided that the inverse Θ^{-1} of the mapping defined by MoLC-equations is continuous at the true log-cumulant vector k^*. Given a parametric family $\{p_\xi(\cdot)\}_{\xi \in \Xi}$, this last statement may be difficult to prove because it involves properties of the inverse mapping Θ^{-1}, for which a closed form expression may not be available. The following theorem provides a weaker consistency condition that may be more convenient in practice, since it only involves the direct mapping Θ, for which a closed form expression is available, by definition, thanks to the Mellin-transform formulation of MoLC.

Theorem 3. *Under Assumptions A, B and C, suppose that Ξ is an open subset of $\mathbb{R}^M$, that Θ is continuously differentiable in Ξ, and that the Jacobian determinant $J_\Theta(\xi)$ is non-zero for all $\xi \in \Xi$. Then, the conclusions of Theorems 1 and 2 hold.*

4.2 Strong consistency for several pdf families

The sufficient conditions discussed in the previous subsection are general and allow stating the (strong) consistency of the MoLC estimators developed for a wide collection of parametric families. Here, we focus more closely on several parametric distributions that have been widely employed in the SAR image-processing literature (see Table 1) and apply the result given by Theorem 3 to demonstrate the strong consistency of MoLC estimates for these distributions. In the statements of this section we consider that Assumption B holds or, in other words, that only samples reporting admissible sample log-cumulants are considered. We will investigate the restrictions given by Assumption B later (see Section 5).

Corollary 1. *MoLC estimates for the GΓD distribution are strongly consistent.*

The proofs of this and the following corollaries are given in Appendix B.

Noticing that the Weibull ($\kappa = 1$), Gamma ($\nu = 1$) and Nakagami ($\nu = 2$) distributions are subfamilies of the GΓD family we immediately obtain the following.

Corollary 2. *MoLC estimates for the Weibull, Gamma and Nakagami distributions are strongly consistent.*

As can be easily seen in Table 1 some pdf families allow formulating an explicit analytical continuous inverse of MoLC equations and, therefore, we obtain the following.

Corollary 3. *MoLC estimates for the lognormal and heavy-tailed Rayleigh distributions are strongly consistent.*

Finally, we demonstrate the strong consistency for the remaining several pdf families.

Corollary 4. *MoLC estimates for the Fisher distribution are strongly consistent.*

Corollary 5. *MoLC estimates for the K and K-root distributions are strongly consistent.*

Thus, when applicable (Assumption B), MoLC provides strongly consistent estimates for all the pdf families in the selection of Table 1. We stress that this is an important theoretical justification for the previously developed methods employing these estimates, including [16, 23].

5   Applicability of MoLC estimates

As concluded in the experimental studies in the literature and further supported by the attractive analytical properties established in Section 4, MoLC can be a suitable option, once the classical alternatives ML and MoM fail to provide feasible estimators either due to high complexity of expressions, or to infinite moments. However, as can be readily seen in Table 1, MoLC has its own limitations, originating from the possible noncompatibility of the system of MoLC equations with the observed sample log-cumulants $\hat{k}$.

In this section we investigate the problem of the applicability of several pdf-families to model the sample data. The applicability conditions will be formulated in terms of log-cumulants and, as such, also represent the applicability conditions of MoLC to parameter estimation for these families. These conditions have been explored previously in the form of $\hat{k}_2 \sim \hat{k}_3$ diagrams in [8, 5, 17] for Fisher, Nakagami, K and GΓD distributions. In this report our aim is to give analytical conditions on the sample $\hat{k}$ to identify the applicability of MoLC to specific families. In other words, we seek to formulate explicitly the condition given by Assumption B in Section 4 for several distribution families. We stress that such conditions have not been formulated in the literature and, however, are crucial in practice, as will be demonstrated in Section 7, in order to verify whether the MoLC method can be employed for a specific sample. We will concentrate on the GΓD and K pdf families, obtaining the analytical applicability conditions for the Fisher and K-root distribution families as well.

In order to obtain the MoLC estimates for the GΓD distribution the following equation needs to be solved (see Table 1):

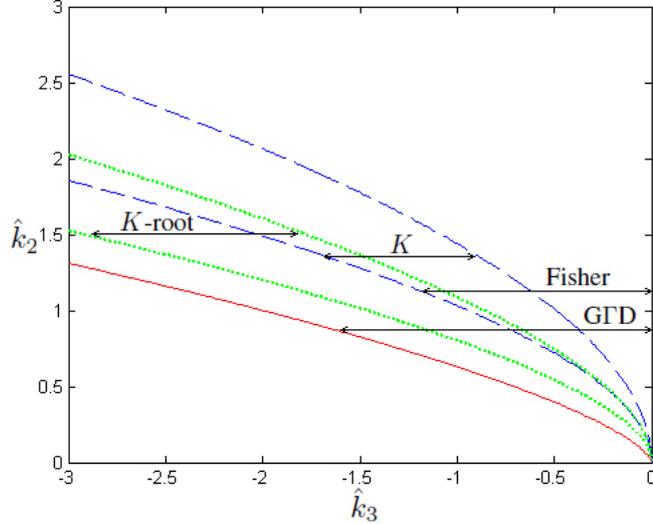$$\frac{\hat{k}_2^3}{\hat{k}_3^2} = \frac{\Psi^3(1, \kappa)}{\Psi^2(2, \kappa)} \tag{6}$$

Figure 1: $\hat{k}_2 \sim \hat{k}_3$ diagram for GΓD, Fisher, K and K-root distributions.

where $\Psi(n, x)$ denotes the n-th order polygamma function [18]. As demonstrated in Appendix C, the right hand side is continuous and monotonously increasing to infinity (as $\kappa \to \infty$) with $\lim\limits_{\kappa \to 0} \frac{\Psi^3(1, \kappa)}{\Psi^2(2, \kappa)} = 0.25$. Therefore, the MoLC system of equations is compatible for samples reporting

$$\hat{k}_2 \geqslant 0.63 \, |\hat{k}_3|^{2/3}. \tag{7}$$

This represents the applicability condition of MoLC to GΓD.

Regarding now the approximative solution developed in [17], where (6) was solved based on the second order approximation of polygamma functions [18], we consider the direct numerical approach considered in this report preferable for the following two reasons. First, the approximation involved in [17] holds as $\kappa \to \infty$ which can be a wrong assumption in general case[3]. Second, the approximative method [17], originating from the Cardano's formula, can only be applied when $\hat{k}_2^3 / \hat{k}_3^2 \geqslant 0.375$, which is slightly more restrictive than the limitation given by (7).

The applicability of MoLC estimates to K-distributed samples is analyzed in Appendix C. The following conditions on $\hat{k}$ are obtained:

$$\begin{cases} \hat{k}_3 < 0 \\ \Psi[1, \Phi_2(\hat{k}_3)] < \hat{k}_2 \leqslant 2\Psi\left[1, \Phi_2\left(\frac{\hat{k}_3}{2}\right)\right] \end{cases} \tag{8}$$

where $\Phi_2(x)$ denotes the inverse of $\Psi(2, x)$.

---

[3]More specifically, in multilook SAR image processing the value $(\kappa\nu - 1)$ of GΓD corresponds to the shape parameter L of the gamma distribution (see Table 1), which represents the number of looks parameter that lies characteristically in range $[1, 8]$. Therefore, since $\kappa = \nu^{-1}[L + 1]$, one may expect to observe small values of κ for $\nu > 1$.

When MoLC is employed to estimate the parameters of the K-root distribution [4, 16] its applicability conditions are given by:

$$\begin{cases} \hat{k}_3 < 0 \\ \frac{1}{4}\Psi[1, \Phi_2(8\hat{k}_3)] < \hat{k}_2 \leqslant \frac{1}{2}\Psi[1, \Phi_2(4\hat{k}_3)] \end{cases} . \tag{9}$$

Finally, the restriction of MoLC applicability to the Fisher pdf family is written as:

$$\hat{k}_2 \geqslant \Psi[1, \Phi_2(-|\hat{k}_3|)]. \tag{10}$$

We note that there is no restriction on the sign of $\hat{k}_3$ since the third MoLC equation allows arbitrary values of $\hat{k}_3$.

The derivation of these last two restrictions (9) and (10) can be performed analogously to that of the K distribution.

In Fig. 1 the applicability restrictions (7)-(10) are presented visually in the form of $\hat{k}_2 \sim \hat{k}_3$ diagram, $\hat{k}_3 < 0$. The comparison of the Fisher distribution's applicability restriction (10) with that of K-law (8) confirms a significantly wider applicability of the Fisher family established in [5, 19]. On the other hand, comparison of GΓD and Fisher restrictions confirms a wider range of applicability of GΓD [17].

6 Synthetic-data experiments

In this section we proceed with new synthetic data experiments for the GΓD and K distribution families. We concentrate on these two families since we consider them to be important for image processing applications, see [3, 21, 6], and the estimation of their parameters with MoLC to be less studied in the literature.

6.1 Generalized gamma distribution

Table 2: Average and MSE of the GΓD parameter estimates and the averaged KS-distance between the true and the estimated pdfs over 10 independently generated samples obtained by MoLC, SISE and ML for samples of sizes 250, 1000 and 5000. Last column reports the average computation time (in milliseconds) for the sample size 5000.

$(\nu^*, \kappa^*, \sigma^*)$	Method	$N = 250$			$N = 1000$			$N = 5000$			
		Average	MSE	KS	Average	MSE	KS	Average	MSE	KS	T
(2, 2, 1)	MoLC	(2.16, 2.22, 1.01)	(0.25, 0.58, 0.10)	0.065	(2.00, 2.12, 0.99)	(0.10, 0.39, 0.05)	0.066	(1.99, 2.04, 0.99)	(0.09, 0.05, 0.05)	0.057	7
	SISE	(1.92, 2.43, 0.91)	(0.24, 0.59, 0.12)	0.069	(1.98, 2.17, 0.97)	(0.18, 0.32, 0.06)	0.063	(2.08, 1.89, 1.05)	(0.12, 0.09, 0.05)	0.060	225
	ML	(1.95, 2.34, 0.93)	(0.19, 0.41, 0.11)	0.070	(1.95, 2.20, 0.96)	(0.11, 0.25, 0.04)	0.063	(2.05, 1.94, 1.03)	(0.10, 0.17, 0.03)	0.055	372
(0.5, 5, 0.5)	MoLC	(0.54, 4.80, 1.23)	(0.02, 1.12, 1.02)	0.081	(0.50, 5.21, 0.73)	(0.01, 0.98, 0.17)	0.081	(0.49, 5.17, 0.49)	(0.00, 0.81, 0.11)	0.076	8
	SISE	(0.56, 4.61, 1.44)	(0.04, 1.91, 1.36)	0.080	(0.52, 5.20, 0.86)	(0.01, 1.32, 0.22)	0.084	(0.51, 5.22, 0.48)	(0.02, 0.62, 0.15)	0.075	261
	ML	(0.54, 4.69, 1.20)	(0.01, 2.09, 0.81)	0.092	(0.51, 5.22, 0.74)	(0.01, 1.11, 0.11)	0.087	(0.49, 4.87, 0.48)	(0.00, 0.76, 0.09)	0.076	353
(3, 0.75, 2)	MoLC	(2.98, 0.93, 1.85)	(0.40, 0.10, 0.11)	0.046	(2.97, 0.84, 1.91)	(0.14, 0.02, 0.20)	0.044	(2.87, 0.82, 1.92)	(0.09, 0.01, 0.01)	0.037	7
	SISE	(3.59, 0.67, 2.10)	(0.35, 0.06, 0.05)	0.047	(2.97, 0.78, 1.97)	(0.11, 0.01, 0.12)	0.050	(3.16, 0.70, 2.05)	(0.05, 0.01, 0.02)	0.042	194
	ML	(3.35, 0.77, 2.01)	(0.42, 0.08, 0.07)	0.041	(2.92, 0.81, 1.94)	(0.10, 0.02, 0.19)	0.041	(3.10, 0.72, 2.04)	(0.04, 0.01, 0.01)	0.038	445

Contrary to its fairly well explored subfamilies such as gamma, Weibull and lognormal distributions, GΓD pdf family remains largely an open field for parameter estimation research. This owes to the fact, that both classical MoM and ML parameter estimation techniques bring to systems of highly non-linear ill-behaved systems of equations [24, 25, 3] that do not allow the use of classical numerical estimation approaches, such as, e.g., Newton-Raphson (NR) approach which reported persistent divergence in a panel of cases [26, 25]. Once the appropriate converging techniques are defined different initializations bring the ML estimator to distinct minima of the likelihood function whereas the further study of their respective consistency poses yet another challenging problem [3]. In light of these problems, various alternative techniques have been explored to obtain ML estimates including parameter space reduction [24], root isolation [25], trial and error [27] and model augmenting to four-parameters [28] approaches. In case of GΓD, the MoM parameter estimation technique does not give solution to the problem, since MoM also leads to a system of highly nonlinear equations [27, 29]. Their solution involves cumbersome numerical procedures such as iterative root-finding algorithms, and, in general, their comparative performance is weak [29, 17]. Another critical side of MoM estimates is that their theoretical properties, such as existence, uniqueness and consistency are yet to be established. To address some of these issues, a modification of the classical MoM approach has been proposed in [3] that suggests the use of fractional order moments and allowed to reformulate the unfeasible system of MoM equations in a more accessible way. More specifically, a scale-independent shape estimation (SISE) procedure was developed in [3], that enabled to obtain one implicit non-linear equation for the shape parameter ν. It has been demonstrated that the SISE method is globally convergent and brings to consistent GΓD parameter estimates.

In this section we analyze the use of MoLC to the GΓD parameter estimation problem. Sample configurations were generated by the inverse transform sampling (via numerically approximated incomplete gamma function). The analysis of the obtained samples suggests that sample configurations violating the restriction (7) arise rarely (in our study, in around 2% of cases), yet persistently for different parameter configurations on the considered sample sizes. In the following, whenever such samples are encountered, the GΓD model is replaced by the best fitting (in terms of likelihood) GΓD subfamily, i.e. by either gamma, lognormal or Weibull distribution, whose applicability is universal in terms of log-cumulants.

In light of the above mentioned GΓD-specific parameter estimation difficulties, we compare the MoLC techniques with two benchmark approaches: 1) ML and 2) SISE. Contrary to MoLC, both benchmark approaches require appropriate initialization. We notice that although the global convergence of SISE has been proved in [3] we have observed some poor convergency cases which might be due to small sample sizes[4]. Thus, in order to provide as good initialization as possible we have employed the MoLC estimates as the first approximation for the NR numerical solution procedures involved in SISE (with shape equation $\mathcal{S}$, see in [3]) and ML (we assumed the MoLC initialization to fall close enough to the true estimate so that NR can converge locally). The estimation was performed for the three sample sizes: $N = 250$, $N = 1000$ and $N = 5000$.

---

[4]More specifically, in some cases we have observed the convergence of the shape parameter ν to zero starting with very accurate initialization. In the following experimental study, we have removed the underlying sample configurations for the fairness of comparison.
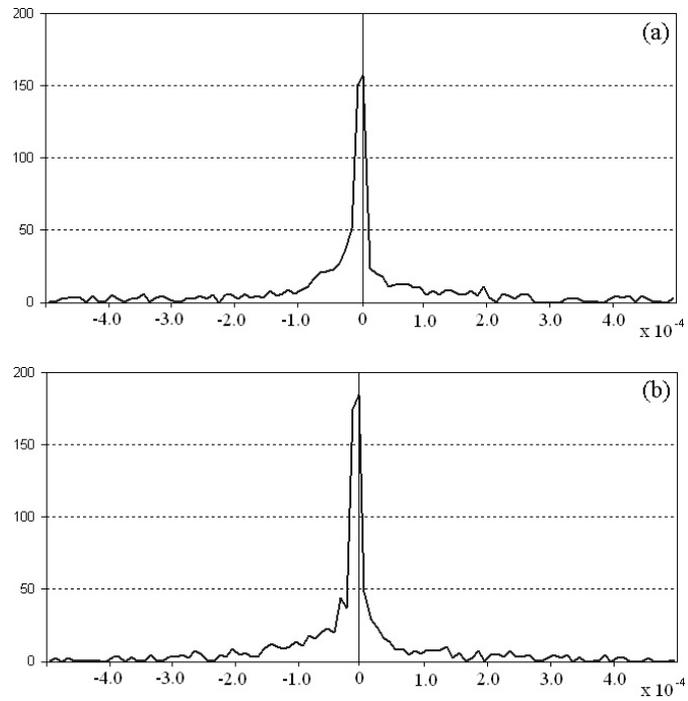
Figure 2:   Histograms of (a) {SMSE(MoLC) - SMSE(SISE)} and (b) {SMSE(MoLC) - SMSE(ML)} collected over 1000 independent samples of size $N = 1000$ with random configurations of parameters (ν, κ, σ).

The sampling and the respective estimation procedures were rerun 10 times and Table 2 presents the averages and the mean square errors (MSE) of the obtained estimates (compared to the true parameter values) over the performed 10 runs. Overall, MoLC estimates provided very competitive results that can in some cases be further refined by ML approach. Analyzing the SISE approach we can state the comparable accuracy of results as reported by MoLC. In order to further compare the performance of the estimation approaches we bring attention to several critical issues: first, the applicability, second, the sensitivity of the estimators while operating with small sample sizes, and finally their computational complexity. We have always observed the ML convergence (NR procedure) initialized via MoLC which confirms the good MoLC accuracy in light of the generally unreliable behavior of ML approach to GΓD [25, 3]. It is worth noticing that the resulting two stage MoLC+ML approach constitutes a consistent estimator since both components have this property [2]. MoLC estimates demonstrated good competitive performance on small samples which became less pronounced with large sample sizes, especially as compared to ML which is largely known to be the best performing large sample estimator [30]. Finally we can state the best computational performance demonstrated by MoLC, and especially so on larger sample sizes since this estimator does not involve iterative sample statistics reestimation: This is demonstrated in th last column of Table 2 where we report the average computational times obtained on a Dual-core 1.83GHz, 2Gb RAM, WinXP system for the considered estimators on the sample size $N = 5000$. Further still, the polygamma and inverse polygamma functions numerical estimations involved in MoLC are fast and stable given the regular behavior of both functions.

We now comment on some large MSEs observed during the estimation process (see Table 2). We feel that it does not purely owe to the small sample sizes involved, but also reflects an inherent feature of the GΓD parameter estimation. More specifically, as has been observed in [24, 27], the GΓD pdf family is flexible to the point where substantially different parameter configurations can bring to close pdf shapes which renders the small sample parameter estimation procedure critically sensitive. To address this problem we estimate the obtained Kolmogorov-Smirnov (KS) distances

$$\text{KS} = \max_{x>0} \left| F(x) - F^*(x) \right|$$

where F and F^* are the estimated and the true GΓD cumulative distribution functions, respectively. This distance represents one of the classical statistical tools to characterize the divergence between random variables [22]. Indeed, the values of KS distance allow to appreciate the accuracy of pdf estimation as a function, see Table 2. To present consistent results the obtained estimates have been averaged out over 10 runs.

To further evaluate the comparative performance of MoLC, we report the sample-based MSE (SMSE) estimation accuracy comparison generalizing the Nakagami pdf estimation analysis performed in [5]. More specifically, on 1000 independent samples $\{x_i\}$ of size $N = 1000$ each for the three considered methods we have calculated

$$\text{SMSE} = \frac{1}{N} \sum_{i=1}^{N} \left| p(x_i) - p^*(x_i) \right|^2$$

where p and p^* are the estimated and the true GΓD pdfs, respectively, and constructed the histograms of {SMSE(MoLC)-SMSE(SISE)} (Fig. 2(a)) and {SMSE(MoLC)-SMSE(ML)} (Fig. 2(b)). For each sample, the scale parameter was fixed to $\sigma = 1$ and the shape parameters ν and κ were chosen randomly (uniformly on $[0.5, 50]$). The analysis of the histograms (their bias to the negative side) reports slightly lower level of variances (in the form of SMSEs) achieved by MoLC.

The performed synthetic data experiments suggest MoLC to be a competitive alternative to ML and MoM whose principle advantages are the fast and stable computational procedure and the absence of initialization problem.

6.2 K distribution

Here we examine the applicability of MoLC parameter estimation strategy to the 3-parameter K-law distribution, which has been shown to represent the statistics of scattered signals at a diverse set of scales extending to both radar and sonar imagery [12], as well as some further applications (see, e.g., [6]). The pure ML strategy cannot be applied directly to this distribution since the derivative of the modified Bessel function of the second kind K_ν with respect to its index does not allow an analytical expression. The Expectation-Maximization approximative iterative approach was used to address this problem in [31] and reported acceptable results for large sample sizes at the price of a heavy computational complexity. Similar conclusions were obtained with the other ML-approximation methods, for more details see [6]. Therefore, in most real applications with not excessively large size samples available and when the computational complexity is critical the MoM approaches might be preferable [6, 32]. These techniques, however, suffer from a nonzero probability that the moment equations are not invertible [6]: This occurs when the randomness inherent in the sample moments results in a moment ratio greater than the maximum theoretical value, which corresponds to a Rayleigh-distributed envelope. That means that for some samples the MoM approach turns out to be inapplicable to the K distribution. As discussed in Section 5, MoLC approach is also restricted to samples that comply with (8), however, contrary to MoM, the respective applicability conditions are explicitly formulated in (8).

We present the comparison of the MoLC technique with the method of fractional moments (fMoM) that suffers from the same limitations as MoM (being its generalization) but demonstrates lower variances than MoM [32]. We consider the comparison with ML-based techniques for K-law outside of the scope of this study since we experimentally analyze foremost the small sample estimation performance, which is critically weak for ML-approaches to K [6]. In Table 3 the results of MoLC and fMoM parameter estimation for K-law with several parameter configurations are presented. K-distributed samples were obtained via inverse transform sampling thanks to K-law representation as a product of two independent gamma-distributed random variables with parameters $(1, L)$ and (μ, M) [12]. As with GΓD, three sample sizes were considered and for each size the estimation process was rerun 10 times. Table 3 presents the average (over 10) estimates and the MSE between the estimates and the true parameter values.

For this comparison the samples for which either MoLC or fMoM failed to be applicable were not considered in this study. To analyze more the severeness of the applicability limitation given by (8) we generated 1000 K-distributed

Table 3: Average $(\bar{L}, \bar{M})$ and MSE $(\hat{L} - L^*, \hat{M} - M^*)$ of the K-law (with $\mu^* = 100$, L^*, M^*) parameter estimates over 10 independently generated samples obtained by MoLC and fMoM ($\nu = -0.75$) for samples of sizes 250, 1000 and 5000

(L^*, M^*)		(2, 10)		(1, 20)	
Sample	Method	Average	MSE	Average	MSE
$N = 250$	MoLC	(2.21, 11.26)	(0.18, 2.17)	(1.23, 18.81)	(0.18, 3.21)
	fMoM	(2.15, 7.92)	(0.11, 2.31)	(0.82, 18.21)	(0.21, 3.54)
$N = 1000$	MoLC	(2.11, 9.41)	(0.09, 1.57)	(0.88, 21.12)	(0.09, 2.32)
	fMoM	(1.75, 9.40)	(0.10, 1.87)	(1.13, 18.92)	(0.11, 2.71)
$N = 5000$	MoLC	(2.04, 9.90)	(0.02, 1.13)	(1.09, 20.51)	(0.02, 1.44)
	fMoM	(1.98, 11.12)	(0.01, 1.10)	(1.06, 19.39)	(0.02, 1.62)

Table 4: GΓD parameter estimates on the ultrasound image on training sets of size N with obtained KS distances and classification accuracies

N	Class 1 (black)			Class 2 (white)		
	$(\hat{\nu}, \hat{\kappa}, \hat{\sigma})$	KS	Acc	$(\hat{\nu}, \hat{\kappa}, \hat{\sigma})$	KS	Acc
1862	(0.84, 35.59, 2.86)	0.044	97.91%	(3.08, 2.71, 87.39)	0.056	67.08%
912	(1.25, 25.71, 3.99)	0.044	97.70%	(2.81, 3.06, 77.72)	0.060	68.13%
446	(0.91, 39.47, 1.88)	0.039	97.64%	(1.55, 4.21, 66.04)	0.075	68.55%
218	(1.07, 38.74, 2.15)	0.041	97.41%	(1.60, 4.04, 68.84)	0.070	69.07%
107	(2.72, 41.12, 1.44)	0.048	96.88%	(0.97, 5.42, 61.35)	0.087	67.78%

samples of size $N = 1000$ each and concluded that MoLC approach failed (8) in $t_1 = 172$ and fMoM was not applicable in $t_2 = 154$ cases. That suggests that MoLC is considerably restrictive as applied to K law, which was experimentally observed in [4], and does not solve the problem of standard MoM applicability. For the reason of restricted applicability of both MoLC and fMoM the MSE comparison similar to the one presented in Fig. 2 is not feasible.

This study together with the conclusions obtained in [8] suggest the similar level of accuracy of MoLC and fMoM, with, however, an extra parameter to estimate for fMoM - the order of the lowest order moment employed ν. Furthermore, both methods suffer from occasional inapplicability and, as such, some other more computationally intensive, yet universally applicable K parameter estimation approaches [6] might be preferable.
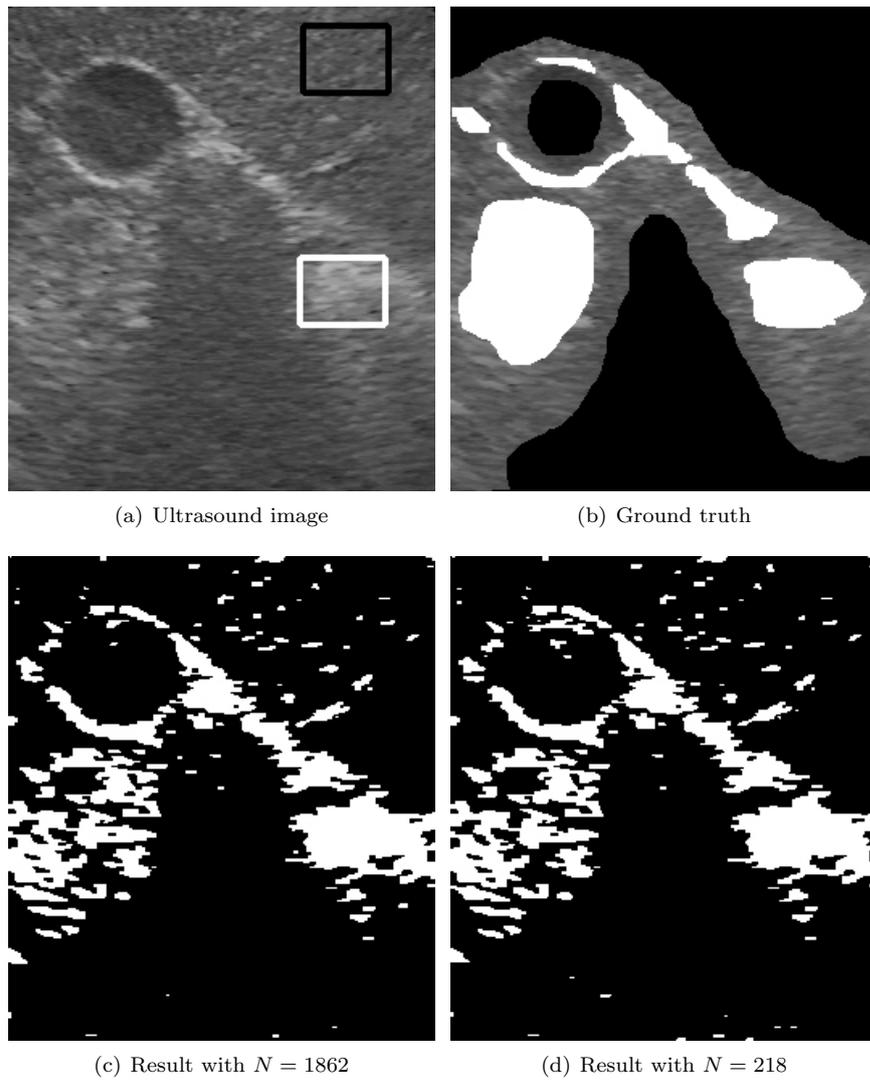
(a) Ultrasound image

(b) Ground truth

(c) Result with $N = 1862$

(d) Result with $N = 218$

Figure 3:   (a) Ultrasound image of gallbladder (with learning areas in rectangles), 250×300 pixels, (b) non-exhaustive ground truth map (white, black - mapped areas, grey tones - no ground truth) and GΓD-based supervised classification results obtained with training samples of sizes: (c) $N = 1862$ and (d) $N = 218$.
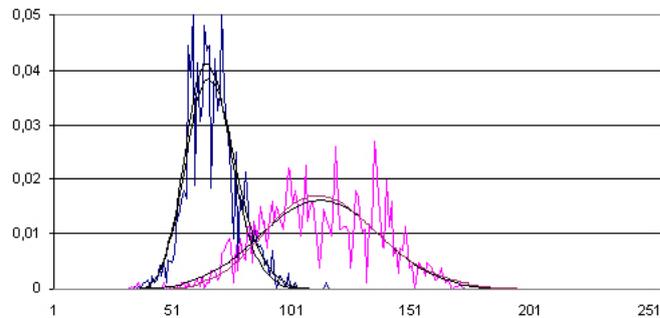
Figure 4: Plots of MoLC-based estimates for the ultrasound image obtained with the GΓD model: normalized histograms of the two considered classes and pdf estimates' plots obtained with samples of sizes $N = 1862$ and $N = 218$.
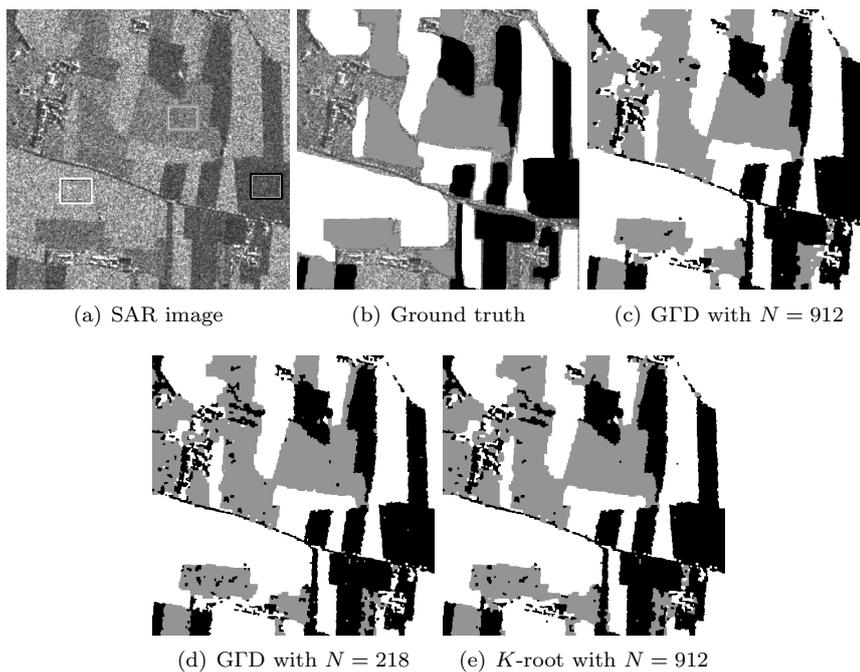

(a) SAR image   (b) Ground truth   (c) GΓD with $N = 912$

(d) GΓD with $N = 218$ (e) K-root with $N = 912$

Figure 5: (a) SAR image of flooded area (with learning areas in rectangles) of Piemonte, Italy (COSMO-SkyMed sensor, ©ASI), 1000×1000 pixels, (b) non-exhaustive ground truth map (white, black, grey - mapped areas, the rest - no ground truth) and supervised classification results obtained with: (c) GΓD model on $N = 912$ samples, (d) GΓD model on $N = 218$ samples and (e) K-root model on $N = 912$ samples.
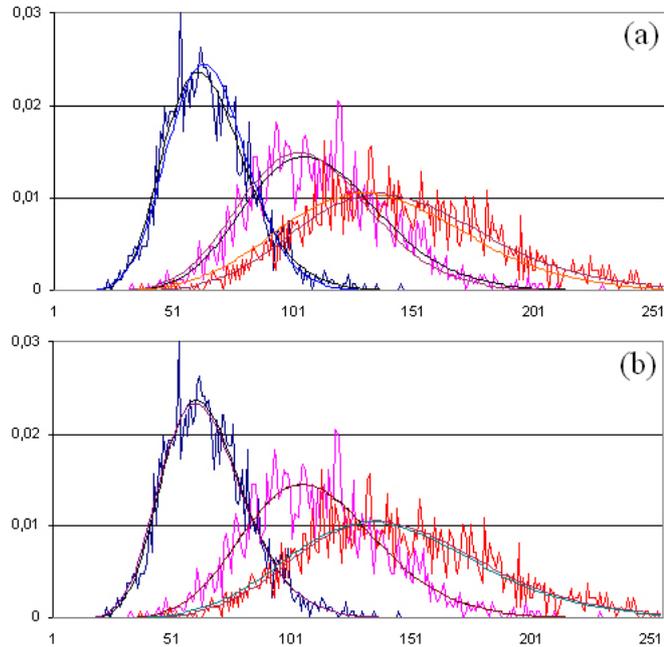
Figure 6: Plots of MoLC-based estimates for the Piemonte image obtained with (a) GΓD model ($N_1 = 1862$ and $N_2 = 218$) and (b) K-root model ($N_1 = 1862$ and $N_2 = 912$). Each graph contains normalized histograms of the three considered classes and pdf estimates' plots obtained with samples of two different sizes.

7 Real-data experiments

In this section we analyze the performance of the MoLC estimator applied to real-data. We notice that comparative performance of MoLC with alternative parameter estimation approaches for most of the pdf families in Table 1 in application to real imagery, and notably for SAR, has been previously tested: for GΓD in [17], Nakagami and Fisher models in [5, 19], GGR in [4], heavy-tailed Rayleigh in [10]. Further relevant MoLC-based mixture estimation experimental results were obtained for SAR pdf modeling in [16], and for SAR image classification in [23]. Therefore, in this section we concentrate on MoLC performance as a function of sample size which we will demonstrate for the GΓD and K families of distribution. The similar study has been performed previously for GGR and reported stable results in terms of correlation coefficient [4].

Table 5: GTD and *K*-root parameter estimates on the Piemonte image on training sets of size N with obtained KS distances and classification accuracies

		Class 1 (black)				Class 2 (grey)				Class 3 (white)		
	N	$(\hat{\nu}, \hat{\kappa}, \hat{\sigma})$	KS	Acc	N	$(\hat{\nu}, \hat{\kappa}, \hat{\sigma})$	KS	Acc		$(\hat{\nu}, \hat{\kappa}, \hat{\sigma})$	KS	Acc
GTD	1862	(1.02, 12.60, 5.67)	0.021	96.19%		(1.21, 7.29, 28.55)	0.019	93.79%		(1.16, 7.47, 33.02)	0.018	95.97%
	912	(1.01, 11.76, 4.81)	0.026	96.07%		(1.07, 9.36, 23.32)	0.034	94.24%		(1.25, 5.25, 40.64)	0.022	96.48%
	446	(1.28, 5.22, 14.24)	0.032	96.16%		(1.29, 5.61, 39.19)	0.035	94.82%		(1.42, 3.38, 47.90)	0.026	97.24%
	218	(1.39, 4.30, 21.19)	0.048	95.58%		(1.34, 4.88, 45.20)	0.029	95.24%		(1.37, 3.64, 50.52)	0.041	97.33%
	N	$(\hat{\mu}, \hat{L}, \hat{M})$	KS	Acc		$(\hat{\mu}, \hat{L}, \hat{M})$	KS	Acc		$(\hat{\mu}, \hat{L}, \hat{M})$	KS	Acc
K-root	1862	(66.63, 5.93, 8.79)	0.022	96.17%		(113.11, 4.80, 23.13)	0.020	93.77%		(149.22, 4.48, 16.39)	0.026	95.77%
	912	(66.12, 4.91, 10.03)	0.025	96.08%		(113.07, 4.85, 21.61)	0.029	93.89%		(146.23, 3.86, 26.36)	0.028	96.51%

In this report, we consider two types of speckled imagery: medical ultrasound and remote sensing SAR, both in application to supervised image classification. To analyze the small sample performance of MoLC we start with training samples of $N \approx 2000$ observations and gradually reduce its size down to $N \approx 200$. First we demonstrate the fit of MoLC estimated pdfs with the normalized histograms and employ the Kolmogorov-Smirnov distance (KS) to quantify the obtained goodness-of-fit. Second, we analyze the MoLC performance in application to supervised image classification as a function of training sample size. To this end we construct classification maps and quantify the obtained accuracy by referring to non-exhaustive ground truth maps. The classification maps are obtained following a likelihood based approach [1] and, therefore, rely directly on the estimated pdf models and serve to characterize the estimation accuracy. In order to take into consideration spatial context in the image and improve the robustness of classification with respect to speckle [13] we employ the Markov random field approach via 2-nd order Potts model, see [1, 23]. The weight coefficient for this single parametric model is set manually based on trial and error method. To minimize the energy of the resulting Gibbs distribution we employ the graph cut approach based on expansion-moves [33, 34, 35].

First we investigate an ultrasound image of gallbladder, see Fig. 3(a). The considered classification is binary and the available non-exhaustive ground truth is presented in Fig. 3(b). The training areas come from the same image, see rectangles in Fig. 3(a) indicating the areas of size $N = 1862$. The first important observation is that for this image both, the Fisher and, consequently, the K model (see Section 5), turned to be inapplicable, same for the fMoM method of K. On the other hand, GΓD model was applicable for all sample sizes. The normalized histograms for both classes along with GΓD pdf estimates' plots on samples of sizes $N_1 = 1862$ and $N_4 = 218$ are presented in Fig. 4. The corresponding parameter estimates with the obtained KS distances are presented in Table 4 for sample sizes from the initial $N_1 = 1862$ to $N_5 = 107$ (at each step, the learning areas were reduced by taking out $\sim 50\%$ of randomly chosen pixels). It is immediate, that the quality of pdf estimation both qualitatively (pdf plots) and quantitatively (KS) remains on the same level going from sample size N_1 to N_4, whereas the actual parameter estimates' values demonstrate some fluctuations. On the last step presented in Table 4 ($N = 107$) the estimation accuracy dropped significantly due to critically small sample size. Fig. 3(c)-(d) present the classification maps obtained with MoLC estimates based on samples of sizes N_1 and N_4, respectively. The visual analysis reports negligible classification difference, and this observation is further confirmed by percentage of correct classification reported in Table 4.

The second set of experiments is conducted on a SAR image obtained by the COSMO-SkyMed satellite system in the Stripmap mode over an agricultural area in Piemonte, Italy (single-look, HH-polarized, 2.5-m ground resolution, 2008), see Fig. 5(a). On this image we investigate the performance of MoLC applied to the GΓD and K models to the supervised three class classification with the manually prepared non-exhaustive ground truth presented in Fig. 5(b). Since the considered image is in the amplitude domain, the K model is replaced by its amplitude equivalent K-root. As with the ultrasound image we start with learning areas of size $N = 1862$ pixels (delimited with rectangles in Fig. 5(a)) and go down to $N = 218$. We first notice that the GΓD model is applicable to all considered sample sizes, whereas reiterating the learning area subsampling

for the K-root model we persistently observed its inapplicability (i.e. failure to comply with restriction (9)) starting from sample size $N = 446$, notably so for class 3. We further report that the Fisher model failed altogether starting from the initial sample size to deal with classes 2 and 3 that reported sample values of $\tilde{k}_2$ and $\tilde{k}_3$ outside of applicability region given by (10). The attempts to solve this problem by changing the location of learning areas did not report success. Plots of pdf estimates obtained for the considered target classes with GΓD and K-root models are presented in Fig. 6, classification maps in Fig. 5(c)-(e), and numerical estimation and classification results are summarized in Table 5.

From these experimental results we conclude that the estimation accuracy of MoLC demonstrates acceptably stable behavior with respect to small sample, and especially for classification purposes, where not the parameter values but rather the histogram fit is of importance. On the other hand the applicability restrictions of MoLC for some pdf families, including Fisher and K distributions, might be critical and need to be constantly verified.

8   Conclusions

In this report we have addressed the problem of pdf parameter estimation by means of the MoLC approach. This recently developed estimator found a wide range of applications, notably for SAR image processing, where the multiplicative nature of the underlying Mellin integral transform allows MoLC to accurately describe advanced texture-speckle statistical product models. We have demonstrated an important statistical property of strong consistency of MoLC estimates for a representative selection of pdf models for which the classical parameter estimators, such as ML and MoM, experience difficulties. For several distribution families, we then derived easy-to-check explicit analytical conditions of MoLC estimator applicability to a given sample to provide a complete picture of MoLC properties. The conducted synthetic-data experiments demonstrated a competitive accuracy of MoLC estimates and a reliable behavior of this estimator for small samples which is a critical issue in applications. Finally, we performed real-data image processing experiments to the problem of supervised classification applied to medical ultrasound and remote sensing SAR imagery. These experiments confirmed the stability of MoLC estimator with respect to sample size and at the same time illuminated the critical side of MoLC given by applicability restrictions.

Based on the Mellin transform, the MoLC approach can be considered as an alternative to MoM that is both more robust to outliers and in some important cases demonstrates better variance properties. On the other hand the issue of MoLC estimator applicability for a specific distribution to a given sample is critical and need to be constantly verified. Applied to a selection of pdf families MoLC enabled to obtain more feasible systems of equations and demonstrated better small sample properties as compared to MoM in situations when the ML approach is not directly applicable. Finally, the analysis performed in this report suggests MoLC, even with its restrictions, to be a valid estimator candidate in case of multiplicative pdf models or when the classical ML and MoM methodologies fail to provide well-established estimators.

Acknowledgments

Appendices

A   Proofs of theorems 1-3

Proof of Theorem 1. Let $\{x_n\}_{n=1}^{\infty}$ be a sequence of independent identically distributed observations $x_n \sim p_{\xi^*}(\cdot)$. To prove the consistency of MoLC, where each estimate $\hat{\xi}_n$ is based on n first observations from $\{x_n\}_{n=1}^{\infty}$, we need to demonstrate the convergence in probability of $\hat{\xi}_n$ to ξ^* as $n \to \infty$, i.e.:

$$\lim_{n \to \infty} \mathbb{P}\left\{ ||\hat{\xi}_n - \xi^*||_{\infty} < \varepsilon \right\} = 1$$

for any $\varepsilon > 0$, where by $||v||_{\infty} = \max_{i=1,\dots,d} |v_i|$ we denote the uniform norm of an d-dimensional vector v.

Define $\Theta : \Xi \to \mathbf{R}^M$ as a mapping of parameter vector ξ into log-cumulants k. Thus, the vector of log-cumulants k^* corresponding to the true parameter values ξ^* may be found as $k^* = \Theta(\xi^*)$.

It is well known that the sample estimates of the log-cumulants $\hat{k}_{sn}$, $s \in \mathbb{N}$, defined by the right hand side of (5) are consistent estimates of the central moments of the random variable $\ln X$ (see [22]).

If we employ now the continuity of mapping Θ^{-1} at $\hat{k}^*$, we obtain the following: for any $\varepsilon > 0$, there exists $\delta_{\varepsilon} > 0$ such that if $||\hat{k} - k^*||_{\infty} < \delta_{\varepsilon}$ and $\hat{k} \in \Theta(\Xi)$, then $||\Theta^{-1}(\hat{k}) - \xi^*||_{\infty} < \varepsilon$. Therefore, if by $||v|| = (v_1^2 + \dots + v_n^2)^{1/2}$ we denote the Euclidean norm of the vector v, then from $||\hat{k}_n - k^*|| < \delta_{\varepsilon}$ follows $||\hat{\xi}_n - \xi^*||_{\infty} < \varepsilon$ or, in other words,

$$\mathbb{P}\{||\hat{\xi}_n - \xi^*||_{\infty} < \varepsilon\} \geqslant \mathbb{P}\{||\hat{k}_n - k^*|| < \delta_{\varepsilon}\}. \tag{11}$$

By applying the Markov and Cauchy-Schwarz inequalities [22], we obtain:

$$\mathbb{P}\{||\hat{k}_n - k^*|| < \delta_{\varepsilon}\} \geqslant 1 - \frac{\mathbb{E}\{||\hat{k}_n - k^*||\}}{\delta_{\varepsilon}} \geqslant 1 - \frac{\left(\mathbb{E}\{||\hat{k}_n - k^*||^2\}\right)^{1/2}}{\delta_{\varepsilon}}.$$

Therefore,

$$\mathbb{P}\{||\hat{\xi}_n - \xi^*||_{\infty} < \varepsilon\} \geqslant 1 - \frac{\left(\mathbb{E}\{||\hat{k}_n - k^*||^2\}\right)^{1/2}}{\delta_{\varepsilon}} = 1 - \frac{\left(\mathbb{E}\{\sum_{s=1}^{M} |\hat{k}_{sn} - k_s^*|^2\}\right)^{1/2}}{\delta_{\varepsilon}} =$$

$$= 1 - \frac{\left(\mathbb{E}\left\{\sum_{s=1}^{M} \left[\hat{k}_{sn} - k_s^* - O\left(\frac{1}{n}\right)\right]^2 + O\left(\frac{1}{n^2}\right)\right\}\right)^{1/2}}{\delta_{\varepsilon}}.$$

We now take into account that [30]

$$\mathbb{E}\hat{k}_{sn} = k_s^* + O\left(\frac{1}{n}\right)$$

and, hence,

$$\mathbb{E}\left[\hat{k}_{sn} - k_s^* - O\left(\frac{1}{n}\right)\right]^2 = \mathbb{E}\left[\hat{k}_{sn} - \mathbb{E}\hat{k}_{sn}\right]^2 = \mathbb{D}\hat{k}_{sn}$$

where $\mathbb{D}X$ denotes the variance of the random variable X [22].

Therefore, we obtain

$$\mathbb{P}\{||\hat{\xi}_n - \xi^*||_\infty < \varepsilon\} \geqslant 1 - \frac{\left(\sum_{s=1}^M \mathbb{D}\hat{k}_{sn} + O\left(\frac{1}{n^2}\right)\right)^{1/2}}{\delta_\varepsilon}.$$

To estimate variances of sample estimates $\hat{k}_{sn}$ defined above we use the following decomposition [30]:

$$\mathbb{D}\hat{k}_{sn} = \frac{m_{2s} - 2sm_{s-1}m_{s+1} - m_s^2 + s^2 m_2 m_{s-1}^2}{n} + O\left(\frac{1}{n^2}\right)$$

where $m_s = \mathbb{E}[\ln X]^s$ are the related true moments, which are finite under Assumption A. Then the following inequality is obtained:

$$\mathbb{P}\{||\hat{\xi}_n - \xi^*||_\infty < \varepsilon\} \geqslant 1 - \delta_\varepsilon^{-1} O\left(\frac{1}{\sqrt{n}}\right) \tag{12}$$

which guarantees the consistency of the estimator. $\square$

Proof of Theorem 2. We first recall that a random sequence $\{\eta_n\}_{n=1}^\infty$ is said to converge to η^* almost surely (a.s.) if

$$\mathbb{P}\{\eta_n \to \eta^*\} = 1.$$

This is equivalent to [30]

$$\forall \varepsilon > 0 : \quad \lim_{n\to\infty} \mathbb{P}\{\sup_{m\geqslant n} |\eta_m - \eta^*| < \varepsilon\} = 1. \tag{13}$$

We recall that sample estimates $\hat{k}_{sn}$ defined in (5) are strongly consistent as central moment estimates for the random variable $\ln X_{\xi^*}$, which follows immediately from the strong law of large numbers [22]. Thus, without the lack of generality (with respect to the probability measure $\mathbb{P}$) we will consider that the following holds everywhere

$$\hat{k}_{sn} \to k_s^* \text{ as } n \to \infty, \ s = 1, \dots, M.$$

It follows immediately, that

$$||\hat{k}_n - k^*||_\infty \to 0 \text{ as } n \to \infty. \tag{14}$$

Then, by employing the continuity of mapping Θ^{-1} we get

$$\mathbb{P}\{\sup_{m\geqslant n} ||\hat{\xi}_m - \xi^*||_\infty < \varepsilon\} \geqslant \mathbb{P}\{\sup_{m\geqslant n} ||\hat{k}_m - k^*||_\infty < \delta_\varepsilon\}.$$

Combined with (14) we obtain

$$\lim_{n\to\infty} \mathbb{P}\{\sup_{m\geqslant n} ||\hat{\xi}_m - \xi^*||_\infty < \varepsilon\} = 1$$

which is equivalent to the strong consistency via (13). $\square$

Proof of Theorem 3. Since Θ is continuously differentiable with non-zero Jacobian over the open connected set Ξ, the inverse-function theorem implies that $\Theta(\Xi)$ is an open set and that Θ is a locally bijective continuously differentiable mapping with continuously differentiable inverse [36]. Since Θ^{-1} exists globally, which is provided by Assumption C, we obtain that Θ^{-1} is continuous on the whole set $\Theta(\Xi)$ and, consequently, also in k^*. This concludes the proof by satisfying the conditions of Theorems 1 and 2. $\square$

B Proofs of corollaries 1-5

Proof of Corollary 1. The GΓD distribution depends on three parameters ν, κ, and σ. Hence, the parameter vector $\xi = (\nu, \kappa, \sigma)$ takes values in $\Xi = (\mathbb{R}^+)^3$ and the mapping Θ from ξ to the vector $\hat{k} = (\hat{k}_1, \hat{k}_2, \hat{k}_3)$ of the first three log-cumulants is given by:

$$\Theta(\xi) = \left(\ln \sigma + \frac{\Psi(0, \kappa)}{\nu}, \quad \frac{\Psi(1, \kappa)}{\nu^2}, \quad \frac{\Psi(2, \kappa)}{\nu^3} \right).$$

The set Ξ is an open subset of $\mathbb{R}^3$, and Θ is injective and continuously differentiable on Ξ, thanks to the properties of the polygamma functions $\Psi(n, x)$, $n \in \mathbb{N}$, $x \in \mathbb{R}^+$ [18]. The Jacobian of Θ can be written as:

$$J_\Theta(\xi) = \frac{1}{\nu^6 \sigma} \Big(3\Psi^2(2, \kappa) - 2\Psi(1, \kappa)\Psi(3, \kappa) \Big), \quad \forall \xi \in \Xi.$$

To prove that J_Θ is nonzero at any point of Ξ, it suffices to show that:

$$\frac{\Psi^2(2, \kappa)}{\Psi(1, \kappa)\Psi(3, \kappa)} < \frac{2}{3}, \quad \forall \kappa > 0.$$

This statement directly derives from the following property of polygamma functions ($\forall \kappa > 0$, $n = 2, 3, \ldots$) [37]:

$$\frac{n-1}{n} < \frac{\Psi^2(n, \kappa)}{\Psi(n-1, \kappa)\Psi(n+1, \kappa)} < \frac{n}{n+1} \tag{15}$$

Therefore, Theorem 3 is applicable to the GΓD distribution. This completes the proof. $\square$

Proof of Corollary 4. Similar to the case of GΓD (see above Corollary 1), all three parameters μ, L and M of the Fisher distribution are positive, i.e., $\xi = (\mu, L, M)$ takes values in the open set $\Xi = (\mathbb{R}^+)^3$. The mapping from these parameters into the first three log-cumulants

$$\Theta(\xi) = \Big(\Psi(0, L) - \Psi(0, M) + \ln(\mu M) - \ln L, \Psi(1, L) + \Psi(1, M), \Psi(2, L) - \Psi(2, M) \Big).$$

is injective and continuously differentiable in Ξ thanks to the differentiability properties of the polygamma functions [18]. The related Jacobian can be written as:

$$J_\Theta(\xi) = -\frac{1}{\mu} \Big(\Psi(2, L)\Psi(3, M) + \Psi(3, L)\Psi(2, M) \Big), \quad \forall \xi \in \Xi.$$

Since $\Psi(2, x) < 0$ and $\Psi(3, x) > 0$ for any $x > 0$ [18], we obtain $J_\Theta > 0$ on Ξ. Therefore, Theorem 3 allows concluding the proof. $\square$

Proof of Corollary 5. All three parameters μ, L and M of the K family are positive and $L < M$, so $\xi = (\mu, L, M)$ takes values in the open set $\Xi = \{(\mu, L, M) \in \mathbb{R}^3 : M > L > 0, \mu > 0\}$. The mapping from these parameters to the first three log-cumulants is:

$$\Theta(\xi) = \Big(\ln\mu + \Psi(0, L) + \Psi(0, M) - \ln LM, \Psi(1, L) + \Psi(1, M), \Psi(2, L) + \Psi(2, M)\Big).$$

Also in this case, the differentiability properties of the polygamma functions imply that Θ is injective and continuously differentiable in Ξ. The Jacobian is given by:

$$J_\Theta(\xi) = \frac{1}{\mu}\Big(\Psi(2, L)\Psi(3, M) - \Psi(3, L)\Psi(2, M)\Big) = \frac{1}{\mu}\frac{\frac{\Psi(2,L)}{\Psi(3,L)} - \frac{\Psi(2,M)}{\Psi(3,M)}}{\Psi(3, L)\Psi(3, M)}, \qquad \forall \xi \in \Xi.$$

To analyze the behavior of $\Psi(2, x)/\Psi(3, x)$ $(x > 0)$, we compute its derivative:

$$\left[\frac{\Psi(2, x)}{\Psi(3, x)}\right]' = \frac{\Psi^2(3, x) - \Psi(2, x)\Psi(4, x)}{\Psi^2(3, x)}.$$

From (15) with $n = 3$ it follows that this derivative is negative for all $x > 0$, and, thus, the function $\Psi(2, x)/\Psi(3, x)$ is decreasing. Since $M > L > 0$, we obtain $J_\Theta > 0$ in Ξ, which with the help of Theorem 3 allows concluding the proof.

By analogy it is easy to prove the strong consistency for the K-root distribution. $\square$

C MoLC applicability conditions

C.1 GΓD family

To study the behavior of the function on the right hand side of (6) we find its derivative

$$\left[\frac{\Psi^3(1, \kappa)}{\Psi^2(2, \kappa)}\right]' = \frac{\Psi^2(1, \kappa)}{\Psi^3(2, \kappa)}\left[3\Psi^2(2, \kappa) - 2\Psi(3, \kappa)\Psi(1, \kappa)\right].$$

Knowing that $\Psi(2, \kappa) < 0$, see [18], and $3\Psi^2(2, \kappa) - 2\Psi(3, \kappa)\Psi(1, \kappa) < 0$, see (15) for $n = 2$, for all $\kappa > 0$, we obtain the monotonous increasing property of the function $\Psi^3(1, \kappa)/\Psi^2(2, \kappa)$. To find its value at $\kappa = 0$, we use the following properties [18]:

$$\kappa \to 0 : \quad \Psi(1, \kappa) \simeq \kappa^{-2} \quad \text{and} \quad \Psi(2, \kappa) \simeq -2\kappa^{-3}.$$

Therefore, $\lim_{\kappa \to 0} \Psi^3(1, \kappa)/\Psi^2(2, \kappa) = 0.25$. Furthermore, [37]

$$\lim_{\kappa \to \infty} \kappa^n \Psi(n, \kappa) = (-1)^{n-1}(n - 1)!$$

And we obtain

$$\frac{\Psi^3(1, \kappa)}{\Psi^2(2, \kappa)} \sim \kappa, \quad \kappa \to \infty.$$

Hence, $\Psi^3(1, \kappa)/\Psi^2(2, \kappa)$ is a continuous monotonously increasing function with values $(0.25, +\infty)$. And, as such, (6) has a unique positive solution whenever:

$$\frac{\hat{k}_2^3}{\hat{k}_3^2} > 0.25.$$

C.2 K-distribution

Given any values of (L, M) the first MoLC equation for K-law (see Table 1) allows to obtain the value of μ. Thus, all restrictions of MoLC applicability for K-distributed samples originate from the expressions for $\hat{k}_2$ and $\hat{k}_3$. The first obvious restrictions are:

$$\hat{k}_2 > 0, \qquad \hat{k}_3 < 0. \tag{16}$$

One further restriction originates from the compatibility of the equations for $\hat{k}_2$ and $\hat{k}_3$. In the following we denote the inverse mapping of $\Psi(1, \cdot)$ as $\Phi_1 : \mathbb{R}^+ \to \mathbb{R}^+$, and of the inverse mapping of $\Psi(2, \cdot)$ as $\Phi_2 : \mathbb{R}^- \to \mathbb{R}^+$. The strict monotonicity and positivity of $\Psi(1, \cdot)$ [18] imply that, if (L, M) $(L < M)$ satisfies the second MoLC equation, then $L > \alpha = \Phi_1(\hat{k}_2)$. Similarly, if (L, M) solves the third equation, then $L > \beta = \Phi_2(\hat{k}_3)$.

Let us first assume that $\alpha \leqslant \beta$. For each $L > \beta$, there exists a unique $M > L$ such that (L, M) solves the third MoLC equation. Let $F : (\beta, +\infty) \to (\beta, +\infty)$ be the mapping from L to the corresponding unique solution M, i.e.:

$$\Psi(2, L) + \Psi[2, F(L)] = \hat{k}_3 \tag{17}$$

and

$$F(L) = \Phi_2[\hat{k}_3 - \Psi(2, L)] \quad \forall L > \beta. \tag{18}$$

Plugging $M = F(L)$ in the second equation, we obtain that $(L, F(L))$ solves the system of MoLC equations if and only if $G(L) = \hat{k}_2$ where $G : (\beta, +\infty) \to \mathbb{R}$ is given by:

$$G(L) = \Psi(1, L) + \Psi[1, F(L)]. \tag{19}$$

Therefore, MoLC admits a solution if and only if $\hat{k}_2$ falls within the range of G. Since, F and G are continuously differentiable on $(\beta, +\infty)$ equations (17) and (19) give:

$$\begin{cases} \Psi(3, L) + \Psi[3, F(L)]F'(L) = 0 \\ G'(L) = \Psi(2, L) + \Psi[2, F(L)]F'(L) \end{cases} \qquad \forall L > \beta$$

and, thus,

$$G'(L) = \Psi(3, L) \left\{ \frac{\Psi(2, L)}{\Psi(3, L)} - \frac{\Psi[2, F(L)]}{\Psi[3, F(L)]} \right\} \quad \forall L > \beta.$$

Thanks to (15) and the strict decreasing of $\Psi(2, \cdot)/\Psi(3, \cdot)$ (see the proof of Corollary 5), the condition $G'(L) > 0$ holds if and only if $F(L) > L$, or, in other words:

$$\hat{k}_3 - \Psi(2, L) > \Psi(2, L).$$

Thus, G is strictly increasing in $\beta < L < \gamma = \Phi_2(\hat{k}_3/2)$, and is strictly decreasing for $L > \gamma$. Since, trivially, $\lim_{L \to \beta} F(L) = +\infty$, $\lim_{L \to +\infty} F(L) = \beta$, and $\lim_{L \to \beta} G(L) = \lim_{L \to +\infty} G(L) = \Psi(1, \beta)$, we obtain that $G(L)$ takes values in the interval $(\Psi(1, \beta), G(\gamma)]$. Since G is a continuous function, the system of MoLC equations admits solution if and only if $\hat{k}_3 < 0$ and:

$$\Psi(1, \beta) < \hat{k}_2 \leqslant G(\gamma),$$

i.e., explicitly:

$$\Psi[1, \Phi_2(\hat{k}_3)] < \hat{k}_2 \leqslant 2\Psi\left[1, \Phi_2\left(\frac{\hat{k}_3}{2}\right)\right]. \tag{20}$$

These bounds were obtained in the case $\alpha \leqslant \beta$, i.e., $\Phi_1(\hat{k}_2) \leqslant \Phi_2(\hat{k}_3)$, which is equivalent to the left inequality in (20). Similarly, also the condition $\hat{k}_2 > 0$ (16) is incorporated in (20).

On the other hand, if the same arguments presented for $\alpha \leqslant \beta$ are repeated for the case $\alpha > \beta$, the same bounds as in (20) are obtained. However, the condition $\alpha > \beta$ is equivalent to $\hat{k}_2 < \Psi[1, \Phi_2(\hat{k}_3)]$ and this condition is incompatible with (20). Therefore, the system of MoLC equations admits no solution when $\alpha > \beta$ and the condition (20) univocally identifies the set of admissible log-cumulant vectors for the K distribution.

References

[1] C. M. Bishop. *Pattern Recognition and Machine Learning.* Springer, New York, 2006.

[2] A. Stuart and J. Keith. *Kendall's Advanced Theory of Statistics.* Wiley, New York, 6th edition, 2008.

[3] K. Song. Globally convergent algorithms for estimating generalized gamma distributions in fast signal and image processing. *IEEE Trans. Image Process.*, 17(8):1233–1250, 2008.

[4] G. Moser, J. Zerubia, and S. B. Serpico. SAR amplitude probability density function estimation based on a generalized Gaussian model. *IEEE Trans. Image Process.*, 15(6):1429–1442, 2006.

[5] C. Tison, J.-M. Nicolas, F. Tupin, and H. Maitre. A new statistical model for Markovian classification of urban areas in high-resolution SAR images. *IEEE Trans. Geosci. Remote Sens.*, 42(10):2046–2057, 2004.

[6] D. A. Abraham and A. P. Lyons. Reliable methods for estimating the K-distribution shape parameter. *IEEE J. Ocean. Eng.*, 35(2):288–302, Apr. 2010.

[7] R. A. Redner and H. F. Walker. Mixture densities, maximum likelihood, and the EM algorithm. *SIAM Review*, 26(2):195–239, 1984.

[8] J.-M. Nicolas. Introduction aux statistiques de deuxième espèce: applications des logs-moments et des logs-cumulants à l'analyse des lois d'images radar. *Traitement du Signal (in French)*, 19(3):139–167, 2002.

[9] B. Epstein. Some applications of the Mellin transform in statistics. *Ann. Math. Stat.*, (19):370–379, 1948.

[10] E. E. Kuruoglu and J. Zerubia. Modelling SAR images with a generalization of the Rayleigh distribution. *IEEE Trans. Image Process.*, 13(4):527–533, 2004.

[11] E. W. Stacy. A generalization of the gamma distribution. *Ann. Math. Statist.*, 33:1187–1192, 1962.

[12] E. Jakeman and P. N. Pusey. A model for non-Rayleigh sea echo. *IEEE Trans. Antennas Propagat.*, 24:806–814, 1976.

[13] C. Oliver and S. Quegan. *Understanding Synthetic Aperture Radar Images.* SciTech, Raleigh, NC, USA, 2nd edition, 2004.

[14] J. W. Shin, J. H. Chang, and N. S. Kim. Statistical modeling of speech signals based on generalized gamma distribution. *IEEE Signal Process. Lett.*, 12(3):258–261, 2005.

[15] J. H. Chang, J. W. Shin, N. S. Kim, and S. K. Mitra. Image probability distribution based on generalized gamma function. *IEEE Signal Process. Lett.*, 12(4):325–328, 2005.

[16] V. A. Krylov, G. Moser, S. B. Serpico, and J. Zerubia. Enhanced dictionary-based SAR amplitude distribution estimation and its validation with very high-resolution data. *IEEE Geosci. Remote Sens. Lett.*, 8(1):148–152, Jan. 2011.

[17] H.-C. Li, W. Hong, Y.-R. Wu, and P.-Z. Fan. On the empirical-statistical modeling of SAR images with generalized gamma distribution. *IEEE J. Sel. Top. Signal Process.*, 5(3):386–397, Jun. 2011.

[18] M. Abramowitz and I. Stegun, editors. *Handbook of Mathematical Functions.* Dover, New York, 1964.

[19] F. Galland, J.-M. Nicolas, H. Sportouche, M. Roche, F. Tupin, and P. Refregier. Unsupervised synthetic aperture radar image segmentation using Fisher distributions. *IEEE Trans. Geosci. Remote Sens.*, 47(8):2966–2972, 2009.

[20] S. N. Anfinsen and T. Eltoft. Application of the matrix-variate Mellin transform to analysis of polarimetric radar images. *IEEE Trans. Geosci. Remote Sens.*, 49(6):2281–2295, Jun. 2011.

[21] T. Eltoft. Modeling the amplitude statistics of ultrasonic images. *IEEE Trans. Med. Imag.*, 25(2):229–240, Feb. 2006.

[22] A. Papoulis. *Probability, Random Variables, and Stochastic Processes.* McGraw-Hill, New York, 3rd edition, 1991.

[23] V. A. Krylov, G. Moser, S. B. Serpico, and J. Zerubia. Supervised high-resolution dual-polarization SAR image classification by finite mixtures and copulas. *IEEE J. Sel. Top. Signal Process.*, 5(3):554–566, Jun. 2011.

[24] J. F. Lawless. Inference in the generalized gamma and log gamma distribution. *Technometrics*, 17:409–419, 1980.

[25] D. R. Wingo. Computing maximum-likelihood parameter estimates of the generalized gamma distribution by numerical root isolation. *IEEE Trans. Reliab.*, 36(5):586–590, 1987.

[26] H. W. Hager and L. J. Bain. Inferential procedures for the generalized gamma distribution. *J. Amer. Statist. Assoc.*, 65:1601–1609, 1970.

[27] A. C. Cohen and B. J. Whitten. *Parameter Estimation in Reliability and Life Span Models.* Marcel Dekker, New York, 1988.

[28] H. Hirose. Maximum likelihood parameter estimation by model augmentation with applications to the extended four-parameter generalized gamma distribution. *Math. Comput. Simul.*, 54:81–97, 2000.

[29] F. Ashkar, B. Bobee, D. Leroux, and D. Morisette. The generalized method of moments as applied to the generalized gamma distribution. *Stochastic Hydrol. Hydraul.*, 2:161–174, 1988.

[30] H. Cramer. *Mathematical Methods of Statistics.* Princeton University Press, Princeton, NJ, 1946.

[31] W. J. J. Roberts and S. Furui. Maximum likelihood estimation of K-distribution parameters via the expectation-maximization algorithm. *IEEE Trans. Signal Process.*, 48(12):3303–3306, Dec. 2000.

[32] D. R. Iskander, A. M. Zoubir, and B. Boashash. A method for estimating the parameters of the k-distribution. *IEEE Trans. Signal Process.*, 47(4):1147–1151, Apr. 1999.

[33] Y. Boykov, O. Veksler, and R. Zabih. Efficient approximate energy minimization via graph cuts. *IEEE Trans. Patt. Anal. Mach. Intell.*, 20(12):1222–1239, Nov. 2001.

[34] V. Kolmogorov and R. Zabih. What energy functions can be minimized via graph cuts? *IEEE Trans. Patt. Anal. Mach. Intell.*, 26(2):147–159, Feb. 2004.

[35] Y. Boykov and V. Kolmogorov. An experimental comparison of min-cut/max-flow algorithms for energy minimization in vision. *IEEE Trans. Patt. Anal. Mach. Intell.*, 26(9):1124–1137, Sep. 2004.

[36] J. R. Munkres. *Analysis on Manifolds.* Addison-Wesley, Reading, MA, 1991.

[37] N. Batir. On some properties of digamma and polygamma functions. *J. Math. Anal. Appl.*, 328(1):452–465, 2007.